

# Lawrence Berkeley National Laboratory

## Recent Work

**Title**

Momentum Aperture of the Advanced Light Source

**Permalink**

<https://escholarship.org/uc/item/4f45h2dk>

**Author**

Decking, W.

**Publication Date**

1998



# ERNEST ORLANDO LAWRENCE BERKELEY NATIONAL LABORATORY

## Momentum Aperture of the Advanced Light Source

W. Decking and D. Robin

**Advanced Light Source Division**

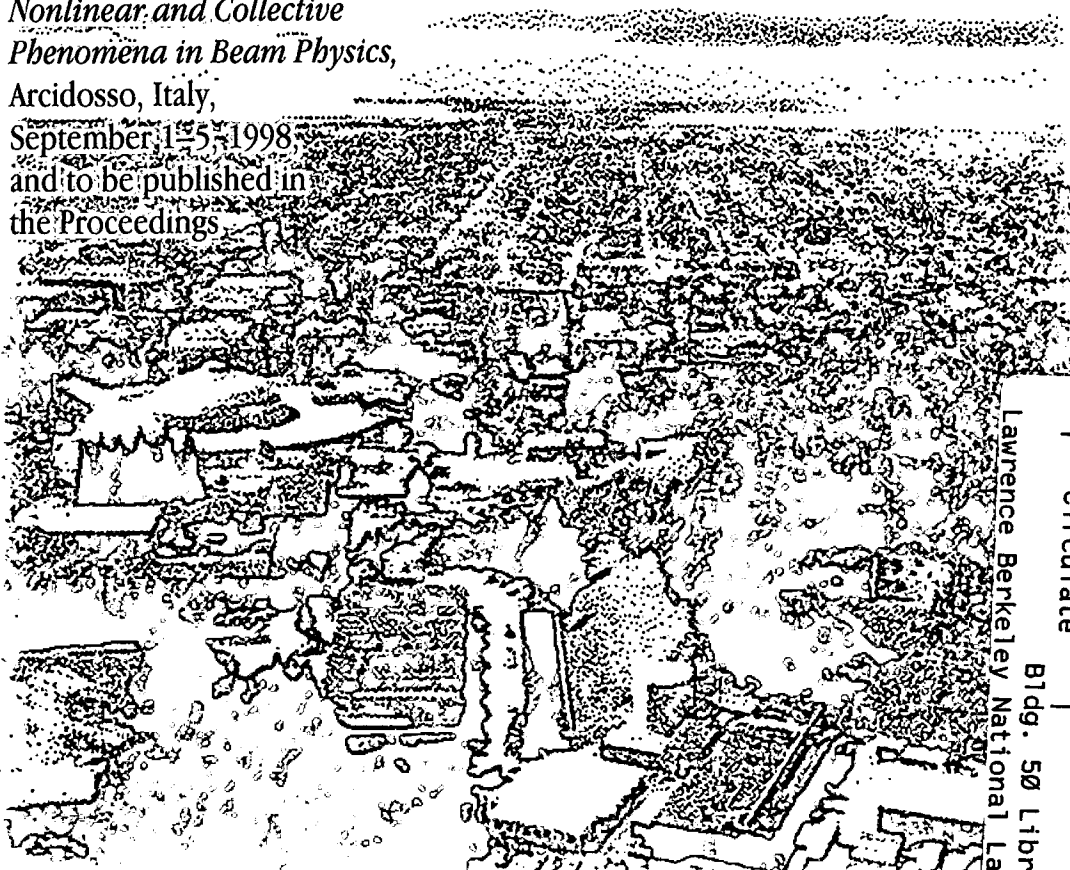
August 1998

Invited paper presented at the  
*16th Advanced ICFA Beam  
Dynamics Workshop on  
Nonlinear and Collective  
Phenomena in Beam Physics,*

Arcidosso, Italy,

September 15, 1998,

and to be published in  
the Proceedings



Lawrence Berkeley National Laboratory

REFERENCE COPY  
Does Not  
Circulate

Bldg. 50 Library - Ref.

Copy 1

LBNL-42462

## **DISCLAIMER**

This document was prepared as an account of work sponsored by the United States Government. While this document is believed to contain correct information, neither the United States Government nor any agency thereof, nor the Regents of the University of California, nor any of their employees, makes any warranty, express or implied, or assumes any legal responsibility for the accuracy, completeness, or usefulness of any information, apparatus, product, or process disclosed, or represents that its use would not infringe privately owned rights. Reference herein to any specific commercial product, process, or service by its trade name, trademark, manufacturer, or otherwise, does not necessarily constitute or imply its endorsement, recommendation, or favoring by the United States Government or any agency thereof, or the Regents of the University of California. The views and opinions of authors expressed herein do not necessarily state or reflect those of the United States Government or any agency thereof or the Regents of the University of California.

## **Momentum Aperture of the Advanced Light Source**

W. Decking and D. Robin

Advanced Light Source Division  
Ernest Orlando Lawrence Berkeley National Laboratory  
University of California  
Berkeley, California 94720

August 1998

# MOMENTUM APERTURE OF THE ADVANCED LIGHT SOURCE

W. Decking and D. Robin

*LBNL, Berkeley, USA*<sup>1</sup>

**Abstract.** This paper shows measurements of the momentum aperture of the Advanced Light Source (ALS) based on Touschek lifetime measurements. The measured data is compared with tracking simulations and a simple model for the apertures will help to explain the observed effects.

## I INTRODUCTION

Particles in a storage ring oscillate about their design orbit. In some cases these oscillations can be irregular or unstable leading to particle losses. The storage ring design must provide a large region around the design orbit in which the oscillations are stable in order to insure good performance of the ring. The envelope of this region in the six-dimensional phase-space is called acceptance. Great effort is spent to increase the acceptance of a storage ring during the design and in operation. A large acceptance is important for two reasons: It facilitates injection into the storage ring and leads to high injection efficiencies, and it elongates the lifetime of the stored particles.

In this paper we describe our efforts to measure the acceptance and compare it with numerical and theoretical predictions. We primarily infer the acceptance from measurements of the Touschek lifetime.

The lifetime of a low energy, small emittance synchrotron radiation source like the ALS is usually limited by the momentum aperture of the ring. The momentum aperture limits the acceptance in the longitudinal direction. Large momentum apertures are reached by

- providing enough rf-voltage for a large bucket
- avoiding the degradation of the momentum aperture due to linear or non-linear synchro-betatron coupling where the particle exceeds the transverse aperture of the machine.

---

<sup>1</sup>) This work was supported by the Director, Office of Energy Research, Office of Basic Energy Sciences, Materials Sciences Division, of the U.S. Department of Energy, under Contract No. DE-AC03-76SF00098.

First we will define the several effects which limit the momentum aperture. Then we show measurements of the dependence of the momentum aperture of the ALS on different working points, chromaticities, and the addition of coupling and insertion devices. We introduce a simple model to explain the momentum dependent dynamic aperture and compare the experimental results and the model with tracking calculations.

## II MOMENTUM APERTURE

The momentum aperture  $\varepsilon$  is the maximum relative momentum deviation  $\delta = \frac{\Delta p}{p_0}$  from the design momentum  $p_0$  a particle can experience without being lost. The momentum aperture is determined by two different processes: the height of the rf-bucket and the maximum stable transverse amplitudes.

The height of the rf-bucket (or rf-aperture) provided by the accelerating voltage in the cavity is

$$\varepsilon_{rf} \propto \pm \sqrt{\frac{V_{rf}}{\alpha h E}}, \quad (1)$$

where  $V_{rf}$  is the rf-voltage,  $\alpha$  the momentum compaction factor,  $h$  the harmonic number, and  $E$  the nominal energy. Equation 1 is only valid for rf-voltages much higher than the energy loss per turn.

The transverse motion of particles is limited by the vacuum chamber aperture. Off-energy particles will oscillate about an off-energy orbit which may be closer to the vacuum chamber wall than the on-energy orbit. Vacuum chamber apertures as well as optical functions vary along the ring. Assuming linear particle motion the largest amplitude a particle can have without hitting the physical aperture is determined by the smallest phase space ellipse fitting through all apertures in the ring,

$$A_{phys,x}(\delta) = \min_{s \in [0,L]} \frac{(x_{vc}(s) - \eta(s)\delta)^2}{\beta_x(s)}, \quad (2)$$

with  $\eta$ ,  $\beta$  being the dispersion and  $\beta$ -function, and  $x_{vc}$  the vacuum chamber aperture. This is termed the physical aperture. Dispersion is usually only present in the horizontal plane, thus the vertical physical aperture is calculated by equation 2 without dispersion, leaving  $A_{phys,y}$  momentum independent.

The particle motion can also reach the vacuum chamber aperture by nonlinear dynamic effects, i.e. the oscillation amplitudes are increased resonantly or chaotically until a particle gets lost. This limit is called dynamic aperture  $A_{dyn}$  and is obtained through tracking calculations or analytical methods. The transverse momentum dependent aperture is given by the minimum of the physical and the dynamic aperture.

When electrons scatter within a bunch, they may transfer enough momentum to be outside the momentum aperture of the storage ring. This effect is called Touschek effect and is proportional to the electron density within a bunch. After a momentum change due to a scattering within the bunch, the particle starts a betatron oscillation around the dispersion orbit. The induced linear invariant amplitude is

$$A_{ind,x}(s, \delta) = H(s)\delta^2, \quad (3)$$

where  $H(s) = \gamma(s)\eta(s)^2 + 2\alpha(s)\eta(s)\eta'(s) + \beta(s)\eta'(s)^2$ . In the presence of linear coupling, the invariant amplitude couples in the vertical plane by  $A_{ind,y}(s, \delta) = \kappa A_{ind,x}(s, \delta)$ .

The induced amplitude should not exceed the maximum allowable transverse amplitude

$$H(s)\delta^2 \leq \min \left[ A_{phys,x}(\delta), A_{dyn,x}(\delta), \frac{1}{\kappa} A_{phys,y}(\delta) \right]. \quad (4)$$

Solving this equation for the maximum  $\delta$  around the ring gives a position dependent momentum aperture, which we call  $\varepsilon_{trans}(s)$ . The absolute momentum aperture is the smaller of  $\varepsilon_{rf}$  and  $\varepsilon_{trans}(s)$  at any position in the ring.

Assuming a flat beam, and thus the main contribution of the velocity spread coming from horizontal motion ( $\sigma'_x$ ), the Touschek lifetime becomes [1]:

$$\frac{1}{\tau_{tou}(s)} \propto \frac{1}{E^3} \frac{I_b}{V_b(s)\sigma'_x(s)} \frac{1}{\varepsilon(s)^2} f\left(\frac{\varepsilon(s)^2}{\sigma'_x(s)^2 E^2}\right). \quad (5)$$

$I_b$  is the bunch current and  $V_b$  the bunch volume. As bunch volume as well as momentum aperture vary around the ring, the Touschek lifetime has to be averaged around the ring <sup>2</sup>.

Figure 1 shows a comparison of the maximum allowable apertures and the induced oscillation amplitudes at different locations in the ALS. The thin lines represent the induced amplitudes. In the straight section, where there is no dispersion, the induced amplitude is zero, that means the particle will only change its energy but not start a betatron oscillation. In the arc section with finite dispersion the induced amplitude shows the quadratic behavior as can be seen from equation 3. The thick lines represent the various apertures. The vertical lines show the rf-aperture with  $\varepsilon_{rf} = 0.03$ , corresponding to the presently available rf-voltage. The dashed-dotted lines show the physical apertures  $A_{phys,x}$  and  $A_{phys,y}$ , where a

---

<sup>2</sup>) A. Nadji et al [2] and others pointed out that the straight forward application of the above formulas leads to wrong results for large momentum deviations. Strong sextupoles lead to higher order dispersion which alters the off momentum closed orbit. In addition, the Twiss functions also vary with the beam energy, thus changing the  $H(s)$  function into  $H(\delta, s)$ . However, at the ALS the linear, momentum independent calculations of the optical functions and the closed orbit vary only up to 5 % for momentum deviations of up to 5 %.

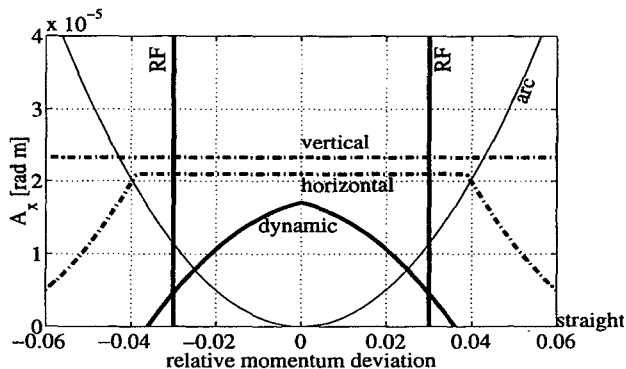


**FIGURE 1.** Contributions of the different aperture effects to the total momentum aperture. The thin lines are the invariant induced amplitudes at different positions in the ring. Dashed dotted lines represent the physical apertures, solid line is the dynamic aperture, and the vertical lines show the rf-aperture.

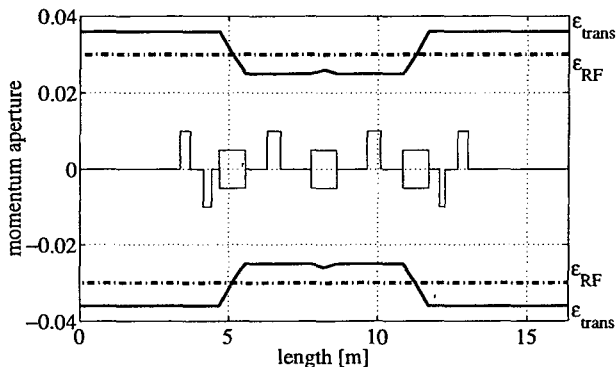


**FIGURE 2.** Momentum aperture along one cell of the ALS storage ring. Solid line is the momentum aperture from transverse limitations as derived from figure 1, dashed-dotted line the rf-aperture.

10 % coupling has been assumed to represent the vertical aperture as a limitation for horizontal motion. The solid line is a sketch of the dynamic aperture for a standard ALS lattice. We will discuss the underlying model in chapter IV. The momentum aperture is defined as the smallest crossing point of the thin and thick lines. As the induced amplitude varies around the ring so does the momentum aperture. Figure 2 shows the momentum aperture for one cell of the ALS. The solid line is the momentum aperture due to transverse limitations as derived from figure 1. The dashed-dotted line is the rf-aperture. In the straight sections the momentum aperture will be defined by the smallest of the rf-bucket height or the dynamic momentum aperture. In the arcs the momentum aperture will be defined by the dynamic momentum aperture, or for large coupling by the vertical physical aperture.



### III MEASUREMENTS OF THE MOMENTUM APERTURE

Measurements of the Touschek lifetime as a function of the rf-voltage were conducted under different storage ring conditions. The synchrotron tune was measured simultaneously, from which one can calculate the bunch length and the rf-bucket height. To enhance the effect of the Touschek scattering over other lifetime effects a high current per bunch was filled in a few equidistantly spaced bunches. The low number of bunches avoids multi-bunch instabilities. The beam conditions thus were 1 mA/bunch and 8 bunches (out of 328) filled.

The data are fitted by applying equation 5 with the following fit parameters: Assuming an initial 1% coupling the bunch volume is corrected by a constant factor that takes into account any volume changes like variation of the coupling, instabilities, etc. The bunch volume is also adjusted according to the changing rf-voltage ( $V_b \propto \sqrt{1/V_{rf}}$ ). The other parameters are the momentum apertures  $\epsilon_{trans}$  in the straight section and in the arc. Thus the data can be fitted with just three parameters. The lines in figures 3 and 4 represent these fits, where the thin lines show the lifetime behavior if there would be no momentum aperture other than the rf-bucket.

Figure 3 left shows measurements of the lifetime with three different settings of the working point. The working point was moved along a line parallel to the  $\nu_x - \nu_y$  coupling resonance. One can clearly see how the momentum aperture and the lifetime improves for higher working points. Figure 3 right displays three measurements with different chromaticities. The higher the chromaticity is set, the lower the momentum aperture.

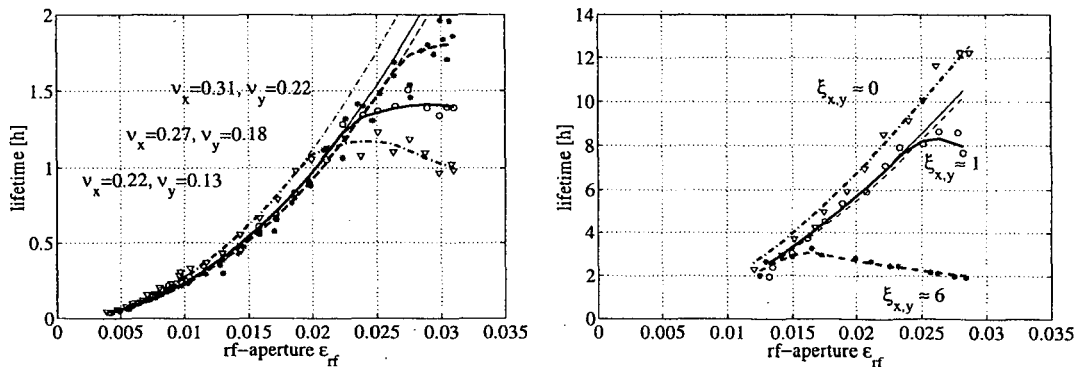


**FIGURE 3.** Beam lifetime as a function of the rf-aperture with three different working points (left) and three different chromaticities (right).

Figure 4 left shows measurements with 1% coupling, while in figure 4 right the coupling was adjusted to  $\approx 10\%$  with the help of skew quadrupoles. In addition a wiggler (2 T peak field, 0.16 m period length, and 3 m total length) was open (circles) or closed (stars) in both cases.

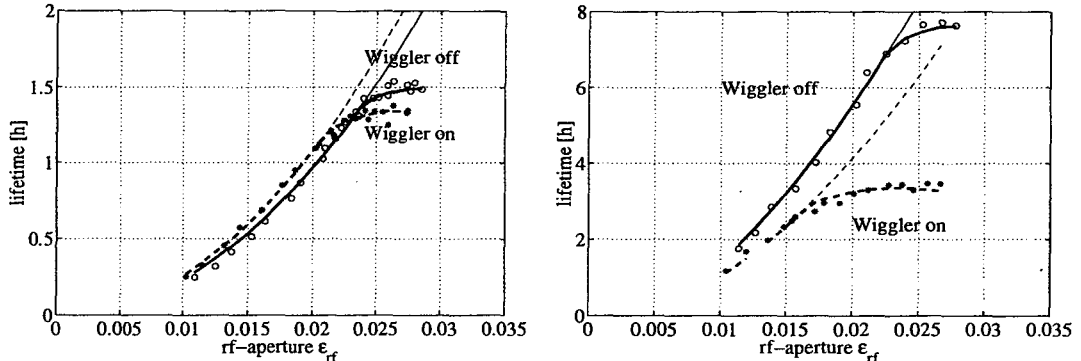


FIGURE 4. Beam lifetime as a function of the rf-aperture with no additional coupling (left) and 10 % coupling (right). In both cases the wiggler was open (circles) or closed (stars).

Table 1 summarizes the results for the measurements shown above as well as for other measurements with different working points and chromaticities.

Let us first consider the cases with no wiggler. In these cases it appears as if the momentum aperture is determined by how close the working point is to the integer resonance  $\nu_y = 8$ . The momentum aperture can be increased by moving the tunes upwards along the coupling resonance  $\nu_x - \nu_y$ , thus increasing the distance to the integer. The momentum aperture decreases with increasing chromaticities according to the larger tune shift with energy in this case, which causes the tune to move more rapidly towards the integer. The introduction of coupling does not change the momentum aperture, which agrees with our measurements of the vacuum chamber apertures.

The cases with the wiggler on show a somewhat different behavior. The momentum aperture is slightly reduced for the low coupling case. Introducing coupling degrades the momentum aperture. Changing the tune upwards along the coupling resonance increases the momentum aperture again. The chromaticities have a similar effect as seen with no wiggler.

## IV SIMPLE MODEL FOR THE DYNAMIC APERTURE

A simple model of the dynamic limit could be as follows: Particles get lost when their tune satisfies a resonance condition. From knowing the tune shift terms with amplitude,  $\frac{\partial \nu_y}{\partial A_x}$ ,  $\frac{\partial \nu_y}{\partial A_y}$ , and energy  $\frac{\partial \nu_y}{\partial \delta}$ ,  $\frac{\partial^2 \nu_y}{\partial \delta^2}$ , one can estimate the tune shift  $\Delta \nu_y$  due to momentum and transverse deviations:

$$\Delta \nu_y = \frac{\partial \nu_y}{\partial A_x} A_x + \frac{\partial \nu_y}{\partial A_y} \kappa A_x + \frac{\partial \nu_y}{\partial \delta} \delta + \frac{\partial^2 \nu_y}{\partial \delta^2} \delta^2 + \dots, \quad (6)$$

where linear coupling is treated as  $A_y = \kappa A_x$ . Setting  $\Delta \nu_y$  as the distance to the closest 'deadly' resonance a momentum dependent dynamic aperture  $A_{dyn,x}(\delta)$  can

be calculated. In figure 5 left measurements of the tune shift with energy are shown together with the model predictions for the vertical tune. The right side displays how the tunes are shifted in tune space.

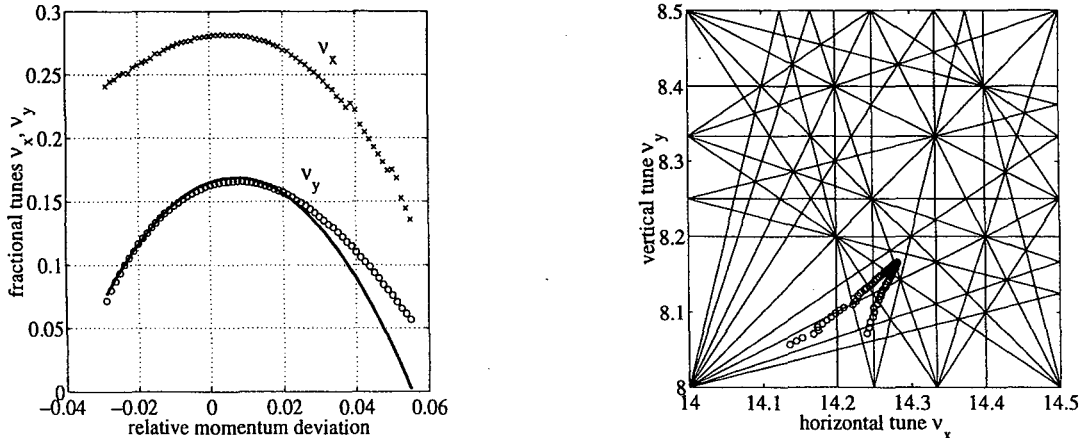


**FIGURE 5.** Measurements of the horizontal (crosses) and vertical (circles) tune shift with energy displayed together with model prediction for the vertical tune (solid line) on the left, and in the tune space on the right.

The dynamic aperture drawn in figure 1 was computed using equation 6 with a tune shift  $\Delta\nu_y = -0.14$ .

## V TRACKING CALCULATIONS

Tracking calculations have been performed to understand the experimental results and prove the accuracy of the model. Particles were tracked through the ALS lattice with a six-dimensional symplectic integrator<sup>3</sup>. The following errors and constraints were included in the model to simulate the realistic machine:

- Physical aperture borders were included in the tracking to prevent particle oscillations outside the realistic vacuum chamber. This is important because large amplitude particles may perform large, but stable oscillations which would be outside the physical aperture but not lead to a loss of the particle in the tracking.
- Linear field errors are simulated according to the optics measurements done at the ALS with the response-matrix fitting method [4]. This errors lead to a  $\beta$ -beat and thus a break in periodicity.
- Random skew quadrupole errors were distributed in all quadrupoles of the lattice and adjusted to obtain a 1% coupling.

<sup>3</sup>) The tracking code TRACY2 was used.

- The wiggler was simulated as a chain of hard-edge bending magnets obtaining the correct linear focusing and longitudinal dynamics properties.

Particles were launched off-energy and off-axis with respect to their off-energy orbit and tracked for 512 turns or until lost (damping times in the ALS are  $\approx 10,000 - 20,000$  turns).

Results for three different tunes and three different chromaticities are shown in figure 6. Also included are the dynamic apertures obtained from the simple model (equation 6) assuming that the vertical tune is shifted towards the integer resonance. The tune shift is adjusted to match the momentum aperture measurements in the arc section of the ring. The thick symbols represent the measured momentum apertures, distributed along the curve showing the amplitude induced by Touschek scattering in the Arc. The agreement between measurement, tracking, and model is quite astonishing.

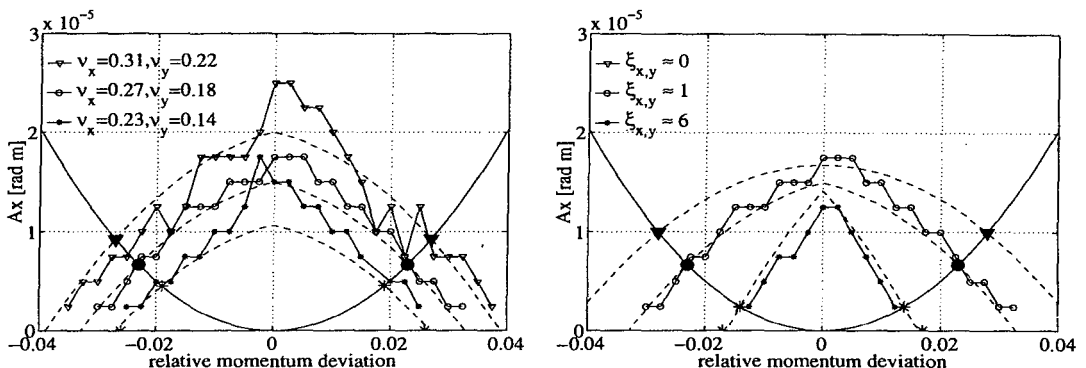


**FIGURE 6.** Maximum stable transverse emittance as a function of momentum deviation. Dashed lines show the dynamic aperture derived from a simple model. The left side is a case with three different working points, while the right side shows three different chromaticities.

Figure 7 shows tracking results for different coupling and wiggler settings. In the left-hand side of figure 7 the tracking was done with the randomly distributed skew-quadrupoles leading to 1% coupling. The wiggler was introduced as mentioned above. The agreement between measurements, tracking, and model again is very good. This situation changes if additional coupling is introduced into the tracking model by means of skew-quadrupole families distributed in the same way as in the ring. The transversal dynamic aperture for particles with smaller energy deviations is greatly reduced, while the dynamic aperture for large momentum deviations is roughly the same as in the low coupling case. The nominal vacuum chamber aperture is still large enough for the 10% coupling case. This means that we either underestimate the linear coupling in the model, do not know the real vacuum chamber apertures well enough, or have a too simple picture of the influence of the skew quadrupoles.

The introduction of the wiggler in the highly coupled case shows at least qualitative agreement between measurement and tracking. The momentum aperture is further reduced. We think this is due to the fact that the periodicity of the lattice

is further destroyed by introducing a wiggler. This allows other resonances to be excited [5], thus changing the distance to the closest 'deadly' resonance. The effect is less visible with small coupling because one still seems to need the coupling fields to excite large vertical oscillations which will hit the small gap vacuum chambers.

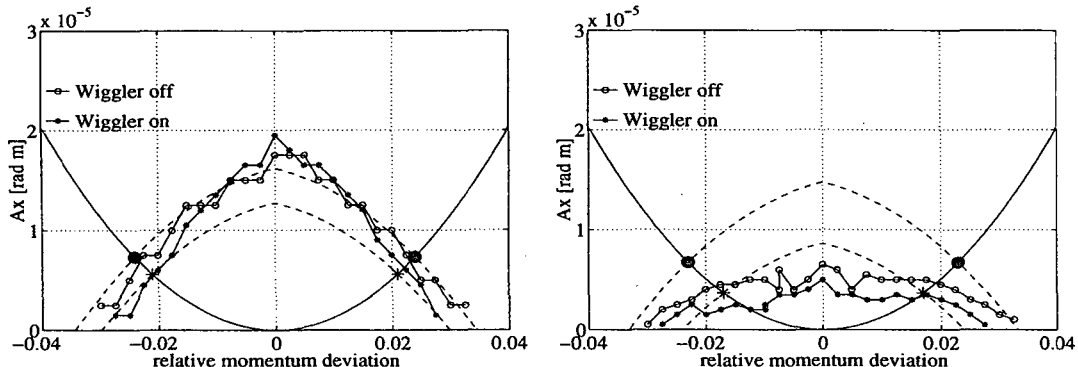


**FIGURE 7.** Maximum stable transverse emittance as a function of momentum deviation. Dashed lines show the dynamic aperture derived from a simple model. The left side is a case with low coupling, while the right side shows the case with additional coupling.

Table 1 summarizes the measurements and the tracking calculations for the cases mentioned throughout this text. It also shows if the tracking and the simple model agree qualitatively.

**TABLE 1.** Measured and calculated momentum aperture in the straight and in the arc section for different machine conditions.

$\kappa$	$\xi_{x,y}$	$\nu_x$	$\nu_y$	measured $\epsilon$ [%]	calculated <sup>a</sup> $\epsilon$ [%]	agreement		
				straight	arc	tracking-model		
Wiggler off								
0.01	1.0	0.31	0.22	>3.2	2.7	3.9	2.8	yes
0.01	1.0	0.27	0.18	>3.3	2.4	3.3	2.4	yes
0.01	1.0	0.22	0.13	2.6	2.0	2.8	1.9	yes
0.01	0.0	0.27	0.18	>2.8	2.8			
0.01	6.0	0.27	0.18	1.7	1.4	1.6	1.3	yes
0.10	1.0	0.27	0.18	>2.8	2.3	3.0	1.8	no
Wiggler on								
0.01	1.0	0.27	0.18	>3.3	2.1	3.0	2.1	yes
0.10	1.0	0.27	0.18	>2.8	1.6	2.8	1.6	no
0.10	0.0	0.27	0.18	>2.8	1.7			
0.10	6.0	0.27	0.18	1.8	1.3			
0.10	1.0	0.31	0.22	>3.2	1.9	3.5	2.0	no

<sup>a</sup> Momentum deviation where dynamic aperture from tracking equals induced amplitude

The reduction of the momentum aperture with wiggler and skew-quadrupoles is a disturbing effect for standard ALS operations. Usually the vertical beam size is enlarged by additional coupling to get a longer beam lifetime. To overcome this

problem, the tune has been changed away from what we believe are the disturbing resonances. The momentum aperture (and thus the lifetime) improved, as can be seen in table 1. Further analysis, especially with the frequency analysis methods [6] should allow to predict which resonances are excited in the special cases.

## VI CONCLUSION

Through measurements of the Touschek lifetime we are able to derive the momentum aperture of the Advanced Light Source. We find that the momentum aperture is not entirely determined by the rf-aperture ( $\varepsilon_{rf}$ ). Also the physical apertures are large enough (for coupling up to 10%) that they do not limit the momentum aperture. The aperture is defined by dynamic effects, which are only partially described by our models. It is important to understand these dynamic limits to improve the lifetime in the ALS and accurately predict the lifetime (and dynamic aperture) in future machines.

## REFERENCES

1. H. Bruck, *Accélérateurs Circulaires de Particules* (Presses Universitaires de France, Paris, 1966).
2. A. Nadji et al., in *Proc. Particle Accelerator Conference, Vancouver, 1997*, p. 1517.
3. W. Decking et al., in *Proc. European Particle Accelerator Conference, Stockholm, 1998*, p. 1262.
4. D. Robin et al., in *Proc. European Particle Accelerator Conference, Sitges, 1996*, p. 971.
5. D. Robin, J. Safranek, and W. Decking, submitted to *Phys. Rev. ST Accel. Beams*.
6. J. Laskar and D. Robin, *Particle Accelerators* **54**, (1996), p. 185-192.

ERNEST ORLANDO LAWRENCE BERKELEY NATIONAL LABORATORY  
ONE CYCLOTRON ROAD | BERKELEY, CALIFORNIA 94720